

## Transient Increase of the Energy Gap of Superconducting NbN Thin Films Excited by Resonant Narrow-Band Terahertz Pulses

M. Beck,<sup>1</sup> I. Rousseau,<sup>1</sup> M. Klammer,<sup>1</sup> P. Leiderer,<sup>1</sup> M. Mittendorff,<sup>2,3</sup> S. Winnerl,<sup>2</sup> M. Helm,<sup>2,3</sup> G. N. Gol'tsman,<sup>4</sup> and J. Demsar<sup>1,5</sup>

<sup>1</sup>*Department of Physics and Center for Applied Photonics, University of Konstanz, D-78457, Germany*

<sup>2</sup>*Institute of Ion Beam Physics and Materials Research, Helmholtz-Zentrum Dresden-Rossendorf, P.O. Box 510119, 01314 Dresden, Germany*

<sup>3</sup>*Technische Universität Dresden, 01062 Dresden, Germany*

<sup>4</sup>*Moscow State Pedagogical University, Moscow, Russia*

<sup>5</sup>*Ilmenau University of Technology, Institute of Physics, D-98693 Ilmenau, Germany*

(Received 21 September 2012; published 26 June 2013)

Observations of radiation-enhanced superconductivity have thus far been limited to a few type-I superconductors (Al, Sn) excited at frequencies between the inelastic scattering rate and the superconducting gap frequency  $2\Delta/h$ . Utilizing intense, narrow-band, picosecond, terahertz pulses, tuned to just below and above  $2\Delta/h$  of a BCS superconductor NbN, we demonstrate that the superconducting gap can be transiently increased also in a type-II dirty-limit superconductor. The effect is particularly pronounced at higher temperatures and is attributed to radiation induced nonthermal electron distribution persisting on a 100 ps time scale.

DOI: [10.1103/PhysRevLett.110.267003](https://doi.org/10.1103/PhysRevLett.110.267003)

PACS numbers: 74.78.-w, 74.25.N-, 74.40.Gh, 78.47.D-

Nonequilibrium superconductivity has been an intriguing phenomenon in modern solid state physics since the 1960s [1]. The first nonequilibrium effects were observed following injection of quasiparticles through tunnel barriers, or by (quasi)continuous microwave, phonon, or laser irradiation [1,2]. One fascinating observation was the enhancement of the superconducting (SC) gap in Al and Sn under illumination with electromagnetic radiation at subgap frequencies [3]. Subsequent theoretical work identified two mechanisms for the superconducting gap enhancement, quasiparticle (QP) redistribution [4] and enhanced recombination of excited QPs [5]. With subgap excitation, the total QP number is conserved while the low-energy QPs are excited to higher energies. Since low-energy QPs interfere with Cooper pairs more effectively than the high energy ones, the SC gap (and condensate density) can thus be enhanced [4]. Moreover, as the rate of QP recombination into Cooper pairs increases with excess QP energy [5,6], subgap pumping can even decrease the total number of QPs, further amplifying superconductivity [5,6].

With the advent of femtosecond laser technology and novel real-time techniques, time-dependent studies of nonequilibrium phenomena on elementary time scales have become available. The discovery of high- $T_c$  superconductivity in cuprates and pnictides has given a further boost to the field of nonequilibrium SC. Past time-resolved studies explored the dynamics of the SC state [7–12], the interplay between the SC gap and the pseudogap [7,10], the SC-normal phase transition [13–15], and the modulation of the order parameter [16–20].

In this Letter, we study the dynamics of a BCS superconductor following excitation with intense, narrow-band, picosecond, terahertz (THz) pulses. As opposed to excitation with near-infrared (NIR) pulses at 1.55 eV, where carriers are excited from deep below to far above the Fermi level ( $E_f$ ), and the SC state is perturbed only when QPs reach states near the SC gap through a rapid QP-QP and QP-phonon relaxation [9,11,15], THz pumping enables direct excitation of the particles relevant to SC, that is those within the Debye energy of  $E_f$ . We have studied the temperature and excitation density dependence of THz transmission dynamics in a NbN thin film following excitation with intense narrowband (< 3% bandwidth) THz pulses. We demonstrate transient amplification of superconductivity, which is particularly pronounced at temperatures close to  $T_c$ . The results imply that narrow-band pumping generates a long-lived ( $\sim 100$  ps), highly non-thermal QP distribution resulting in amplification of SC that would be washed out under continuous excitation. Importantly, the enhancement effects are observed even in the case of above gap excitation, where QP excitation competes with standard Cooper pair breaking.

The sample used in this investigation was a 15 nm-thick NbN film ( $T_c = 15.4$  K), deposited on a 1 mm thick MgO substrate [21]. It was thoroughly characterized using linear THz spectroscopy [9]. Time-resolved studies of dynamics following THz pumping were performed at the free electron laser (FEL) facility at the Helmholtz-Zentrum Dresden-Rossendorf, which provided intense narrow-band (spectral width  $\approx 30$  GHz, pulse length  $\tau_{\text{FEL}} \approx 18$  ps) THz pulses at a repetition rate of 13 MHz. Experiments were carried out in a standard single color

pump-probe configuration (see the Supplemental Material [22]) at frequencies slightly above ( $\nu_{>} = 2.08$  THz) and slightly below ( $\nu_{<} = 1.26$  THz) the low-temperature gap frequency  $2\Delta/h = 1.5$  THz [9]. The THz beam was split into an intense pump and a weak probe beam, and the time delay between the two ( $t_d$ ) was controlled by a mechanical delay stage. The transmission (Tr) and the photoinduced changes in transmission ( $\delta\text{Tr}$ ) were measured using a liquid helium-cooled bolometer and a lock-in amplifier while modulating at 233 Hz (see the Supplemental Material [22]). We characterized the temporal characteristics of THz pulses using intensity autocorrelation, while the beam profiles were recorded with a pyroelectric camera (see the Supplemental Material [22]).

Figure 1(a) presents the measured  $T$  dependence of Tr through NbN-on-MgO using narrow-band pulses. The data are well reproduced by transfer matrix calculation [23] (dashed lines) using the complex THz conductivity  $\sigma(\omega)$  of NbN measured with single-cycle pulses [9] and measured THz pulse characteristics (see the Supplemental Material [22]). Despite the excellent agreement, the absorbed energy density ( $A$ ) is known only to within 40% absolute accuracy [24]; this variation is due to the combination of uncertainties in the substrate thickness (etalon phenomena), spot diameter, and THz wavelength. The high repetition rate of the FEL source leads to observable continuous heating, increasing the film temperature ( $T$ ) beyond that of the cold finger ( $T_0$ ) (see the Supplemental Material [22]). The continuous heating has been experimentally determined and taken into account (see the Supplemental Material [22]); the temperature ( $T$ ) always

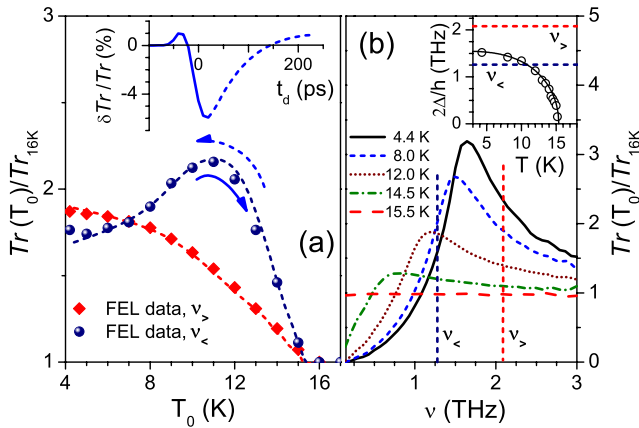


FIG. 1 (color online). (a) Transmission intensity Tr as a function of  $T_0$  as measured at 1.26 THz (circles) and 2.08 THz (diamonds), respectively. Dotted lines are the calculated values obtained by transfer matrix method. Inset to (a) presents the expected  $\delta\text{Tr}/\text{Tr}$  for the data recorded at  $\sim 10$  K and  $\nu = 1.26$  THz, whereby the gap is reduced on the resolution limited time scale (solid line) and recovers on the 100 ps time scale (dashed)—see also the corresponding arrows in the main panel. (b)  $T$  dependence of Tr from the broadband measurements, with the extracted  $T$  dependence of the SC gap shown in the inset.

refers to the effective film temperature, slightly higher than  $T_0$ .

Before discussing results obtained by THz pumping, let us review the recent systematic NIR pumping study on NbN [9]. It was demonstrated that following excitation with a femtosecond near-infrared pulse, the time evolution of the SC gap  $\Delta(t_d)$  in NbN can be directly measured by recording the time evolution of  $\sigma(\omega)$  [9]. It was shown that a few picoseconds after excitation,  $\sigma(\omega)$  can be described by an effective gap  $\Delta^*$  corresponding to an effective temperature  $T^*$  such that  $\Delta^* = \Delta(T^*)$ . This is in accordance with the so-called  $T^*$  model for a nonequilibrium SC [25,26] in which the populations of QPs, Cooper pairs, and high-energy ( $\hbar\omega > 2\Delta$ ) phonons are in quasiequilibrium at an elevated  $T^*$  with respect to the (ambient) temperature of the low-energy ( $\hbar\omega < 2\Delta$ ) phonons [27,28].

Figure 2 summarizes the results obtained by THz pumping at  $\nu_{>} = 2.08$  THz. Figure 2(a) shows traces of the relative transmission change,  $\delta\text{Tr}(t_d)$ , for several absorbed energy densities ( $A$ ) at  $T_0 = 4.3$  K. Here  $A$  was determined from the measured incoming THz pulse energy and  $\sigma(\omega)$  [9]. Following a rapid decrease in Tr on a resolution limited ( $\approx 30$  ps) time scale the SC state recovery proceeds on the 100 ps time scale in agreement with NIR pumping experiments [9]. To determine the absorbed energy density required to deplete SC ( $A_{\text{dep}}$ ) the maximum changes in transmission are converted into corresponding changes in  $\Delta$ . Here the  $T^*$  model is assumed to be valid, so that at  $t_d \approx 30$  ps the SC can be described by  $\Delta^* = \Delta(T^*)$ . Using

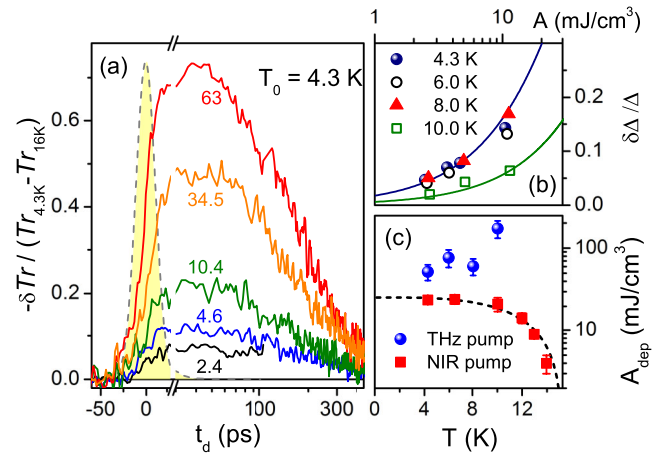


FIG. 2 (color online). (a) Dynamics of the transmission change  $\delta\text{Tr}$  (normalized to  $\text{Tr}_{4.3\text{K}} - \text{Tr}_{16\text{K}}$ ) when pumping with 2.08 THz pulses of different absorbed energy density  $A$  (in  $\text{mJ}/\text{cm}^2$ ). The shaded region presents the pump-probe intensity autocorrelation. (b) The maximum gap reduction  $\delta\Delta/\Delta$  as a function of  $A$  for different temperatures. Solid lines are simple saturation fits (see text). (c) The extracted SC depletion energy density  $A_{\text{dep}}$  as a function of  $T$ , measured with NIR (1.55 eV) [9] and THz (2.08 THz) pumping. The dashed line represents  $E_{\text{cond}}(T) \propto \Delta^2(T)$ .

$\Delta(T)$  [9] the fractional change of the SC gap is obtained via  $\delta\Delta/\Delta = 1 - \Delta^*/\Delta$ .

Figure 2(b) shows  $\delta\Delta/\Delta(A)$  recorded at several temperatures and a fit to a simple saturation model,  $\delta\Delta/\Delta = 1 - \exp(-A/A_{\text{dep}})$ . In Figure 2(c) the extracted depletion energy densities,  $A_{\text{dep}}$ , are compared to the ones obtained by NIR pumping [9]. There,  $A_{\text{dep}}$  was found to be comparable to the SC condensation energy  $E_{\text{cond}} = 22 \text{ mJ/cm}^3$  [29], and to follow its expected  $T$  dependence:  $E_{\text{cond}}(T) = N(0)\Delta^2(T)/2$ . When pumping with THz,  $A_{\text{dep}}(4 \text{ K})$  is about a factor of two larger ( $\approx 50 \text{ mJ/cm}^3$ ). The discrepancy could be related to the absolute uncertainty in  $A$  [24]. However, in contrast to the expected reduction of  $A_{\text{dep}}$  at higher temperatures, with THz pumping  $A_{\text{dep}}(T)$  dramatically increases with temperature [24]. This observation implies the presence of a process that competes with Cooper pair breaking at higher temperatures. In past continuous-pumping experiments [3], the gap (and critical current) enhancement were similarly peaked near  $T_c$ . This was attributed to radiation induced QP redistribution (shuffling of thermally excited QPs to higher energies) [4,5], the process that becomes relevant only when the density of thermally excited QPs,  $n_T(T) \approx N(0) \times \sqrt{2\pi\Delta k_B T} \exp(-\Delta/T)$ , becomes appreciable. Thus, while at 4 K nearly all of the absorbed energy for  $\nu > 2\Delta/\hbar$  results in pair-breaking, near  $T_c$  excitation of thermal QPs becomes increasingly important [for NbN  $n_T(10 \text{ K}) \approx 1000 \times n_T(4 \text{ K})$ ]. We argue that it is the resulting non-thermal QP distribution that gives rise to SC amplification. For above-gap pumping the resulting SC enhancement competes with the pair-breaking process, the manifestation of which is an increase in  $A_{\text{dep}}$  at higher temperatures.

Since NbN's  $2\Delta/\hbar$  varies from 1.5 THz at 4 K to zero at  $T_c$ , the choice of  $\nu < = 1.26 \text{ THz}$  allows for pumping below, resonant with, and above  $2\Delta$  simply by varying temperature. Figure 3 presents transients of transmission changes at  $\nu < = 1.26 \text{ THz}$  recorded at various temperatures. The incoming excitation fluence was kept constant at its maximum value (pump pulse energy before the cryostat was  $\approx 8 \text{ nJ}$ ) with maximum electric field strengths ( $E_{\text{max}}$ ) in NbN of  $\approx 300 \text{ V/cm}$ . As elaborated below, three different excitation mechanisms can be realized, the dominant one depending on the initial temperature and  $h\nu/2\Delta$  ratio.

For  $T < 10 \text{ K}$  direct pair breaking by absorption cannot take place as  $\nu < 2\Delta/\hbar$ . Moreover,  $n_T$  is rather low; thus, the effect of exciting thermally excited QPs is correspondingly small. The measured  $\delta\text{Tr}/\text{Tr}(t_d)$  traces are consistent with a resolution limited reduction of the gap, followed by recovery on the 100 ps time scale. We attribute this (small) gap reduction to the dynamic pair breaking caused by the acceleration of the SC condensate in an intense oscillating electric field [30]. As opposed to excitation of SC with low-frequency intense electric fields [30,31], no elaborate theory exists for the case of pumping with frequency

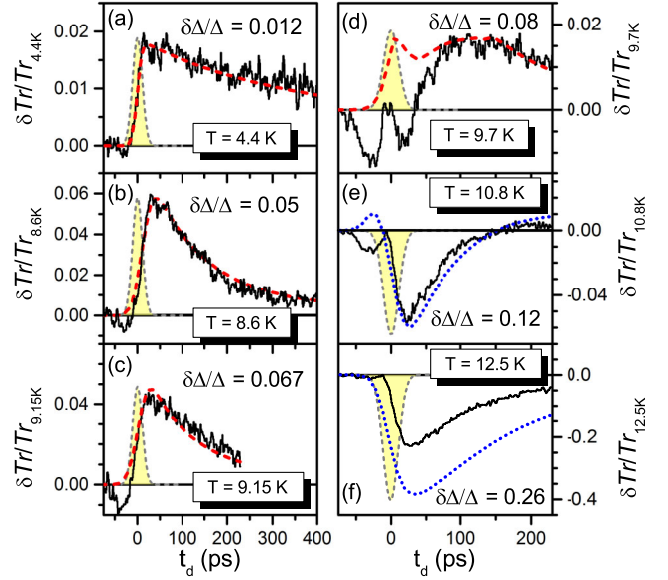


FIG. 3 (color online). Dynamics of the relative transmission change  $\delta\text{Tr}/\text{Tr}$  at  $\nu < = 1.26 \text{ THz}$  recorded at several temperatures. The shaded region presents the pump-probe intensity autocorrelation. For each temperature the maximum relative change in the gap  $\delta\Delta/\Delta$  is calculated from the measured  $\delta\text{Tr}/\text{Tr}$  assuming the  $T^*$  model. The dotted (blue) lines and dashed (red) lines show the predicted  $\delta\text{Tr}/\text{Tr}(t_d)$  based on the  $T^*$  model (see text).

comparable to the inverse pairing time,  $\tau_{\text{pair}}^{-1} = \Delta/\hbar$ . With the NbN carrier density  $n \approx 1 \times 10^{23} \text{ cm}^{-3}$  and the Fermi velocity  $v_f \approx 1.5 \times 10^6 \text{ m/s}$  [32], the maximum super-current density ( $j_{\text{max}} = ne^2 E_{\text{max}}/m\omega$ ) can be contrasted to the depairing current density  $j_d = ne\Delta/mv_f$  [33]. With  $E_{\text{max}} \approx 300 \text{ V/cm}$  we obtain  $j_{\text{max}} \approx 1 \times 10^{13} \text{ A/m}^2$ , which is comparable to  $j_d \approx 6 \times 10^{12} \text{ A/m}^2$ . Thus, the dynamic pair breaking should give rise to a measurable suppression of SC [30] as experimentally observed. The dashed red lines in Fig. 3 are the  $T^*$ -model simulations with the resolution limited pair-breaking time and the ( $T$ -dependent) SC recovery time; the latter was taken from the NIR pumping experiments [9]. Since for  $h\nu < 2\Delta$  no direct pair breaking can take place and no gap reduction due to absorption is expected,  $\delta\Delta/\Delta(t_d)$  was scaled to match the data.

For  $T > 10 \text{ K}$  direct pair breaking is possible since  $2\Delta$  falls below  $h\nu <$ . Here,  $A$  can be determined from  $\sigma(\omega)$ , and the measured transients can be directly compared to the  $T^*$ -model simulation (for  $T > 10 \text{ K}$  the SC recovery time is  $\approx 100 \text{ ps}$  and  $T$  independent [9]). Comparison of simulation (dotted blue lines, no scaling required) with experimental data shows a good agreement (apart from the early time dynamics to be elaborated below). Noteworthy, a similar trend is observed as in the case of pumping with  $\nu >$ , where for higher temperatures the measured  $\delta\Delta/\Delta$  is smaller than the simulated one. This can be



consistently attributed to THz excitation of thermal QPs, whose density is high for  $T > 10$  K.

By far the most dramatic is, however, the behavior in the vicinity of 10 K, where  $h\nu_{<} \lesssim 2\Delta$  while  $n_T$  is already substantial. Because of the nonmonotonic  $T$  dependence of transmission for  $\nu_{<}$  (see Fig. 1)  $\delta\text{Tr}$  is expected to exhibit a nontrivial dynamics in this temperature range—see inset to Fig. 1(a). However, for time delays less than  $\approx 50$  ps the measured traces cannot be reproduced by  $T^*$ -model simulations if THz-pump induced gap reduction (followed by its recovery) is assumed. In fact, for short time delays ( $t_d \lesssim 50$  ps)  $\delta\text{Tr}$  systematically shows the opposite sign to the one predicted. This observation can be attributed to a transient increase of the superconducting gap, whereby the transmission maximum (whose position roughly coincides with  $2\Delta/h$ ) shifts to a higher frequency. The effect is peaked around 10 K, where  $n_T$  is high and  $h\nu \lesssim 2\Delta$ , but its signatures are seen in all of the traces recorded with 1.26 THz pumping.

Within the Eliashberg scenario [2,4–6] the SC gap is enhanced due to the radiation induced changes in the electronic distribution function. In the BCS superconductor the SC gap magnitude and  $T_c$  are obtained by solving the self-consistent BCS gap equation [1,4,6]

$$\Delta = g \int_{\Delta}^{\hbar\omega_c} d\epsilon \frac{\Delta}{\sqrt{\epsilon^2 - \Delta^2}} [1 - 2f(\epsilon)],$$

which is governed by the electron-phonon coupling strength ( $g$ ), cutoff frequency ( $\hbar\omega_c$ ) and the electronic distribution function  $f(\epsilon)$ . Under subgap excitation the number of QP is conserved, yet the QP distribution is transiently modified such that the center of gravity of the distribution function is shifted to energies away from the gap edge. The resulting decrease in the density of the low-lying QPs, which strongly interfere with the condensate, thus leads to an increase of the gap (and the condensate density) [2,4–6]. Naturally, this description is valid only once  $f(\epsilon)$  is well defined. Since any coherent dynamics are expected only on the time scale of the inverse gap frequency ( $\approx 1$  ps) [19], we can safely assume the condition to be met in our case and treat the Eliashberg gap enhancement to be quasi-instantaneous.

In addition, enhanced recombination rate of high energy QP can further boost the gap enhancement by transiently reducing the number of QPs [5]. While QP-QP scattering and QP-phonon scattering processes lead to thermalization of QP distribution they conserve the number of QPs. On the other hand, the pair-wise recombination of QPs by phonon emission and pair breaking by  $\hbar\omega > 2\Delta$  phonon reabsorption do change the QP density. All of the above scattering processes, as well as the phonon escape responsible for recovery [5,6,27,28,34], take place also in thermal equilibrium and their rates are energy dependent [34]. Since the pair recombination is the fastest of these processes [34], and its rate increases with increasing QP energy due to the

larger available phase space (at low QP energies approximately  $\propto \omega^2$ ) [5], this can lead to a transient decrease of the QP density. This way the gap can be further increased during the initial stage of the relaxation process [5]. The QP recombination time can be estimated by  $\tau_R = 1/(Rn_T)$  [27,28], where  $R$  is the bare QP recombination rate. With (average)  $R$  determined by NIR pumping experiments of  $160 \pm 20$  ps $^{-1}$  unit cell [9] and  $n_T(10$  K)  $\approx 2 \times 10^{-4}$  unit cell $^{-1}$  we obtain the upper boundary for  $\tau_R \approx 30$  ps. It follows that this process can be important in NbN, further boosting the gap enhancement.

Gap enhancement has not yet been observed in materials with short electron mean free paths such as NbN. In past experiments with continuous excitation, the absence of gap enhancement was attributed to enhanced QP thermalization [35] due to weak localization [36]. In our experiments, clear signatures of gap enhancement are observed on the 50 ps time scale, the time scale to be compared with the QP-phonon and QP-QP scattering times. The QP-phonon relaxation in a SC is suppressed due to the corresponding coherence factors and is on the order of 100 ps [34]. For QP-QP scattering, Landau-Fermi liquid theory [37] provides an upper bound, as the scattering rate should be increased in impure metals [36]. With  $\tau_{e-e}^{-1} = (\pi^2\sqrt{3}/128)\omega_p[(E - E_f)/E_f]^2$ , taking the plasma frequency  $\omega_p \approx 2-3$  eV [9,38] and Fermi energy  $E_f \approx 3$  eV [38]  $\tau_{e-e}$  is approximately 300 ps. From these estimates it is reasonable to conclude that the nonthermal QP distribution, a foundation for gap enhancement, persists over 100 ps time scale for narrow-band THz pumping.

In order to quantify the gap enhancement, experiments with narrow-band pumping and broadband THz probing are required, together with supporting theoretical simulations of  $\sigma(\omega)$ . From the observed dramatic increase in the SC depletion energy density ( $A_{\text{dep}}$ ) at high temperatures, we conclude that the gap increase up to a factor of  $\approx 2$  can be achieved. Ideally, the pump frequency should be below 1 THz (the lowest frequency at the FEL facility is 1.26 THz). This would enable subgap pumping for temperatures closer to  $T_c$ , where  $n_T$  is large.

To summarize, the effect of resonant pumping of the BCS superconductor NbN is explored using intense narrow-band THz pulses. For high electric fields, the SC state can be suppressed by dynamic pair breaking [30] even when pumping at a frequency less than  $2\Delta/h$ . Upon approaching  $T_c$  the density of thermally excited QPs becomes substantial. Excitation of thermal QPs to higher energies is shown to give rise to a transient gap (and condensate density) increase for subgap pumping. The enhancement effects are present also in the case of above-gap pumping, demonstrated by a dramatic increase in the superconducting state depletion energy at high temperatures. As opposed to past continuous pumping experiments [3], excitation with intense, picosecond THz pulses produces strong enhancement effects even in short

mean-free-path superconductors such as NbN and for pumping frequencies exceeding  $2\Delta/h$ .

This work was supported by the German Israeli DIP Project No. 563363, Alexander von Humboldt Foundation, Ministry of Education and Science of the Russian Federation (Resolution No. 220), Zukunftscolleg, and Center for Applied Photonics at the University of Konstanz. We acknowledge valuable discussions with V. V. Kabanov, A. Leitenstorfer, K. W. Kim, T. M. Klapwijk, V. M. Axt, A. Vagov, and I. Eremin, as well as P. Michel and the FEL team for their dedicated support.

- 
- [1] M. Tinkham, *Introduction to Superconductivity* (McGraw-Hill, New York, 1996), Chap. 11.
- [2] *Nonequilibrium Superconductivity, Phonons, and Kapitza Boundaries*, NATO ASI Series, edited by K.E. Gray (Plenum, New York, 1981).
- [3] A. F. G. Wyatt, V. M. Dmitriev, W. S. Moore, and F. W. Sheard, *Phys. Rev. Lett.* **16**, 1166 (1966); A. H. Dayem and J. J. Wiegand, *Phys. Rev.* **155**, 419 (1967); T. M. Klapwijk, J. N. van den Bergh, and J. E. Mooij, *J. Low Temp. Phys.* **26**, 385 (1977); T. Kommers and J. Clarke, *Phys. Rev. Lett.* **38**, 1091 (1977).
- [4] G. M. Eliashberg, *Pis'ma Zh. Eksp. Teor. Fiz.* **11**, 186 (1970) [*JETP Lett.* **11**, 114 (1970)]; G. M. Eliashberg, S. G. Lisitsyn, and G. M. Eliashberg, *J. Low Temp. Phys.* **10**, 449 (1973).
- [5] J. J. Chang and D. J. Scalapino, *Phys. Rev. B* **15**, 2651 (1977); J. J. Chang and D. J. Scalapino, *J. Low Temp. Phys.* **29**, 477 (1977).
- [6] U. Eckern, A. Schmid, M. Schmutz, and G. Schon, *J. Low Temp. Phys.* **36**, 643 (1979).
- [7] J. Demsar, B. Podobnik, V. V. Kabanov, T. Wolf, and D. Mihailovic, *Phys. Rev. Lett.* **82**, 4918 (1999).
- [8] R. D. Averitt, G. Rodriguez, A. Lobad, J. Siders, S. Trugman, and A. Taylor, *Phys. Rev. B* **63**, 140502(R) (2001).
- [9] M. Beck, M. Klammer, S. Lang, P. Leiderer, V. V. Kabanov, G. N. Gol'tsman, and J. Demsar, *Phys. Rev. Lett.* **107**, 177007 (2011).
- [10] R. A. Kaindl, M. Woerner, T. Elsaesser, D. C. Smith, J. F. Ryan, G. A. Farnan, M. P. McCurry, and D. G. Walmsley, *Science* **287**, 470 (2000).
- [11] A. Pashkin *et al.*, *Phys. Rev. Lett.* **105**, 067001 (2010).
- [12] R. Cortés, L. Rettig, Y. Yoshida, H. Eisaki, M. Wolf, and U. Bovensiepen, *Phys. Rev. Lett.* **107**, 097002 (2011); C. L. Smallwood, J. P. Hinton, C. Jozwiak, W. Zhang, J. D. Koralek, H. Eisaki, D.-H. Lee, J. Orenstein, and A. Lanzara, *Science* **336**, 1137 (2012).
- [13] P. Kusar, V. Kabanov, J. Demsar, T. Mertelj, S. Sugai, and D. Mihailovic, *Phys. Rev. Lett.* **101**, 227001 (2008).
- [14] C. Giannetti, G. Coslovich, F. Cilento, G. Ferrini, H. Eisaki, N. Kaneko, M. Greven, and F. Parmigiani, *Phys. Rev. B* **79**, 224502 (2009).
- [15] M. Beyer, D. Städter, M. Beck, H. Schäfer, V. V. Kabanov, G. Logvenov, I. Bozovic, G. Koren, and J. Demsar, *Phys. Rev. B* **83**, 214515 (2011).
- [16] D. Fausti, R. I. Tobey, N. Dean, S. Kaiser, A. Dienst, M. C. Hoffmann, S. Pyon, T. Takayama, H. Takagi, and A. Cavalleri, *Science* **331**, 189 (2011).
- [17] A. Dienst, M. C. Hoffmann, D. Fausti, J. C. Petersen, S. Pyon, T. Takayama, H. Takagi, and A. Cavalleri, *Nat. Photonics* **5**, 485 (2011).
- [18] K. W. Kim, A. Pashkin, H. Schäfer, M. Beyer, M. Porer, T. Wolf, C. Bernhard, J. Demsar, R. Huber, and A. Leitenstorfer, *Nat. Mater.* **11**, 497 (2012).
- [19] T. Papenkort, V. M. Axt, and T. Kuhn, *Phys. Rev. B* **76**, 224522 (2007); E. A. Yuzbashyan, O. Tsypliyat'yev, and B. L. Altshuler, *Phys. Rev. Lett.* **96**, 097005 (2006); R. Matsunaga, Y. I. Hamada, K. Makise, Y. Uzawa, H. Terai, Z. Wang, and R. Shimano, [arXiv:1305.0381v1](https://arxiv.org/abs/1305.0381v1).
- [20] B. Mansart, J. Lorenzana, A. Mann, A. Odeh, M. Scarongella, M. Chergui, and F. Carbone, *Proc. Natl. Acad. Sci. U.S.A.* **110**, 4539 (2013).
- [21] G. Gol'tsman, O. Okunev, G. Chulkova, A. Lipatov, A. Semenov, K. Smirnov, B. Voronov, A. Dzardanov, C. Williams, and R. Sobolewski, *Appl. Phys. Lett.* **79**, 705 (2001).
- [22] See Supplemental Material at <http://link.aps.org/supplemental/10.1103/PhysRevLett.110.267003> for details on experimental setup, THz pulse characterization, and heating effects.
- [23] B. E. A. Saleh and M. C. Teich, *Fundamentals of Photonics* (Wiley-Interscience, New York, 1991).
- [24] Although the absolute value of  $A$  is given by a large 40% uncertainty, its relative uncertainty as a function of temperature is less than 5%.
- [25] W. Parker, *Phys. Rev. B* **12**, 3667 (1975).
- [26] See, e.g., E. J. Nicol, and J. P. Carbotte, *Phys. Rev. B* **67**, 214506 (2003).
- [27] A. Rothwarf and B. N. Taylor, *Phys. Rev. Lett.* **19**, 27 (1967).
- [28] V. V. Kabanov, J. Demsar, and D. Mihailovic, *Phys. Rev. Lett.* **95**, 147002 (2005).
- [29] C. Geibel, H. Rietschel, A. Junod, M. Pelizzone, and J. Müller, *J. Phys. F* **15**, 405 (1985).
- [30] T. J. Rieger, D. J. Scalapino, and J. E. Mercereau, *Phys. Rev. B* **6**, 1734 (1972).
- [31] W. J. Skocpol, M. R. Beasley, and M. Tinkham, *J. Low Temp. Phys.* **16**, 145 (1974).
- [32] S. P. Chockalingam, M. Chand, J. Jesudasan, V. Tripathi, and P. Raychaudhuri, *Phys. Rev. B* **77**, 214503 (2008).
- [33] D. Dew-Hughes, *Low Temp. Phys.* **27**, 713 (2001).
- [34] S. B. Kaplan, C. Chi, D. Langenberg, J. Chang, S. Jafarey, and D. Scalapino, *Phys. Rev. B* **14**, 4854 (1976).
- [35] E. M. Gershenson, G. N. Gol'tsman, V. D. Potapov, and A. V. Sergeev, *Solid State Commun.* **75**, 639 (1990); P. C. van Son, J. Romijn, T. M. Klapwijk, and J. E. Mooij, *Phys. Rev. B* **29**, 1503 (1984).
- [36] B. I. Altshuler and A. G. Aronov, in *Electron-Electron Interactions in Disordered Systems*, Modern Problems in Condensed Matter Physics Vol. 10, edited by A. L. Efros and M. Pollak (North-Holland, Amsterdam, 1985).
- [37] D. Pines and P. Nozières, *The Theory of Quantum Liquids* (Westview, Boulder, 1999).
- [38] R. Sanjines, M. Benkahoul, C. S. Sandu, P. E. Schmid, and F. Levy, *Thin Solid Films* **494**, 190 (2006); K. Kinoshita, *Phase Transit.* **23**, 73 (1990).